THYROID
Volume 23, Number 8, 2013

DOI: 10.1089/thy.2012.0571

Modulation of Sodium/Iodide Symporter Expression in the Salivary Gland

Krista M.D. La Perle,[1] Dong Chul Kim,[2] Nathan C. Hall,[3] Adam Bobbey,[3] Daniel H. Shen,[4] Rebecca S. Nagy,[5] Paul E. Wakely, Jr.,[6] Amy Lehman,[7] David Jarjoura,[7] and Sissy M. Jhiang[8]

Background: Physiologic iodide-uptake, mediated by the sodium/iodide symporter (NIS), in the salivary gland confers its susceptibility to radioactive iodine–induced damage following ^{131}I treatment of thyroid cancer. Subsequent quality of life for thyroid cancer survivors can be decreased due to recurrent sialoadenitis and persistent xerostomia. NIS expression at the three principal salivary duct components in various pathological conditions was examined to better our understanding of NIS modulation in the salivary gland.
Methods: NIS expression was evaluated by immunohistochemistry in human salivary gland tissue microarrays constructed of normal, inflamed, and neoplastic salivary tissue cores. Cumulative ^{123}I radioactivity reflecting the combination of NIS activity with clearance of saliva secretion in submandibular and parotid salivary glands was evaluated by single-photon emission computed tomography/computed tomography imaging 24 hours after ^{123}I administration in 50 thyroid cancer patients.
Results: NIS is highly expressed in the basolateral membranes of the majority of striated ducts, yet weakly expressed in few intercalated and excretory duct cells. The ratio of ^{123}I accumulation between parotid and submandibular glands is 2.38 ± 0.19. However, the corresponding ratio of ^{123}I accumulation normalized by volume of interest is 1.19 ± 0.06. The percentage of NIS-positive striated duct cells in submandibular salivary glands was statistically greater than in parotid salivary glands, suggesting a higher clearance rate of saliva secretion in submandibular salivary glands. NIS expression in striated ducts was heterogeneously decreased or absent in sialoadenitis. Most ductal salivary gland tumors did not express NIS. However, Warthin's tumors of striated duct origin exhibited consistent and intense NIS staining, corresponding with radioactive iodine uptake.
Conclusions: NIS expression is tightly modulated during the transition of intercalated to striated ducts and striated to excretory ducts in salivary ductal cells. NIS expression in salivary glands is decreased during inflammation and tumor formation. Further investigation may identify molecular targets and/or pharmacologic agents that allow selective inhibition of NIS expression/activity in salivary glands during radioactive iodine treatment.

Introduction

The sodium (Na^+)/iodide (I^-) symporter (NIS) mediates iodide accumulation in the thyroid gland. This basolateral membrane glycoprotein of thyroid follicular epithelial cells couples the inward movement of two Na^+ ions with one I^- ion in an active process driven by a Na^+ gradient established by Na^+/K^+ adenosine triphosphatase. Accordingly, thyroid follicular cells may have an intracellular I^- concentration 20- to 40-fold higher than that in plasma, as I^- is a required component of the thyroid hormones tetraiodothyronine or thyroxine (T_4) and triiodothyronine (T_3). NIS-mediated iodide uptake in the thyroid gland is driven by thyrotropin, and additional thyroid-restricted proteins such as pendrin and thyroid peroxidase facilitate the subsequent transport of I^- to the follicular lumen and its organification respectively. The thyroid gland's ability to concentrate and retain iodide is clinically advantageous because it allows the use of radioactive iodine (RAI) for the diagnosis and treatment of thyroid disease, including thyroid cancer. Various extrathyroidal tissues, including nasopharynx, lacrimal and salivary glands, gastric and colonic mucosae, pancreas, thymus, choroid plexus, and the ciliary body of the eye, also express NIS protein and are capable of accumulating iodide, albeit to a lesser degree (1–3). However, the most clinically relevant expression and uptake are in the salivary gland, the gastric mucosa, and the lactating mammary gland (4).

Departments of [1]Veterinary Biosciences, [3]Radiology, [5]Internal Medicine, [6]Pathology, and [8]Physiology and Cell Biology; [7]Center for Biostatistics; The Ohio State University, Columbus, Ohio.
[2]Department of Pathology, Gyeongsang National University, Jinju, South Korea.
[4]Department of Nuclear Medicine, National Defense Medical Center, Tri-Service General Hospital, Taipei, Taiwan.

Iodide concentration in the salivary gland has been recognized for more than three-quarters of a century. Nevertheless, it wasn't until the cloning of NIS and the development of NIS antibodies that we and others were able to attribute this activity to ductal cells as opposed to acinar cells (2,3). The exact biologic role of iodide in extrathyroidal tissues, including the salivary gland, is unknown. Obvious functions of saliva that are likely independent of iodide include cleansing of the oral cavity, facilitation of mastication, food solubilization, initiation of digestion, bolus formation, lubrication, and mucosal protection by immunoglobulin A (5). In this context, it is interesting to note that studies investigating patterns of dental pathology and dietary differences report low rates of dental caries and a lack of tooth loss in populations residing in iodine-rich geographical locations (6).

Physiologic iodide uptake by the salivary gland confers its susceptibility to RAI-induced damage following administration of ^{131}I for the treatment of thyroid cancer. The quality of life for many thyroid cancer survivors is considerably decreased due to recurrent sialoadenitis, persistent xerostomia, and progressive susceptibility to dental caries and periodontal disease (7–9). In this study, we investigated NIS modulation in salivary glands by examining NIS expression in salivary ductal cells in normal and various pathological conditions. The information acquired may help to develop novel strategies to prevent and/or minimize ^{131}I-induced salivary gland damage in thyroid cancer patients.

Cumulative radioactivity in the salivary gland is the net outcome between NIS-mediated ^{131}I uptake and clearance by saliva secretion. Differential kinetics of radionuclide accumulation between parotid and submandibular glands have been reported (10,11). ^{131}I-induced salivary dysfunction is more often noted in the parotid gland than in the submandibular gland. To investigate the underlying reasons for this discrepancy, we examined and compared the percentage of NIS-positive cells in the parotid gland versus the submandibular gland. We also examined and compared ^{123}I accumulation in the parotid gland versus the submandibular gland by single-photon emission computed tomography (SPECT)/CT imaging of the head and neck 24 hours after ^{123}I administration in 50 thyroid cancer patients prior to their ^{131}I treatment.

Materials and Methods

Human salivary gland tissue microarray construction

Neutral buffered formalin-fixed, paraffin-embedded tissue blocks and hematoxylin and eosin (HE)-stained slides containing salivary glands of various histologic diagnoses were requested through the Ohio State University (OSU) Wexner Medical Center's (WMC) Tissue Archives Service. Access to and use of these samples was covered under an exempt institutional review board (IRB)-approved protocol allowing for use of anonymous archival tissues in research. HE slides were reviewed by two pathologists for confirmation of the original diagnosis. Two representative areas of normal, inflamed, and neoplastic salivary gland tissues from each patient, whenever applicable, were selected for tissue microarrays. Cores (1.5 mm) were placed into the recipient blocks using a precision arraying instrument (Micro Tissue Arrayer; Beecher Instruments, Silver Springs, MD). Three distinct tissue microarray blocks containing a total of 235 cores from 79 cases were constructed.

NIS immunohistochemistry and analysis

Tissue sections (4 μm) placed on positively charged slides were incubated with 3% hydrogen peroxide for five minutes to block endogenous peroxidase. Antigen retrieval was performed by heat-induced epitope retrieval in 1× Target Retrieval Solution (S1699, Dako, Carpinteria, CA) for 25 minutes. Slides were incubated with affinity purified rabbit anti-human NIS polyclonal antibody, p442NIS, 1:40 at room temperature for 60 minutes in a Dako Autostainer Immunostaining System, followed by avidin and biotin block using the Dako Biotin Blocking System (X0590) for 20 minutes. The secondary antibody used was a biotinylated goat anti-rabbit antibody (1:200, BA-1000, Vector Laboratories, Inc., Burlingame, CA) that was incubated for 20 minutes at room temperature. The detection system used was Vectastain Elite (PK-6100, Vector Laboratories, Inc.) used for 30 minutes. Staining was visualized with the 3,3'-diaminobenzidine (DAB) chromogen (K3468, Dako), and slides were counterstained with Richard Allen hematoxylin.

NIS immunostaining was evaluated independently by two investigators in two categories: staining intensity and the percentage of positive cells in assigned cell types. Only the staining intensity in the plasma membrane was assigned into the following semiquantitative grading scheme: 0 = negative, 1+ = mild, 2+ = moderate, and 3+ = marked staining intensity (see Fig. 4 and legend as an example). The percentage of NIS-positive cells in assigned cell types was scored separately in 5%-point increments. For comparison of the relative abundance of NIS-positive ductal cells between cores of submandibular and parotid salivary glands, we superimposed a 20×20 grid with 400 squares on each normal tissue core (Fig. 2A). The number of squares overlying the core area (333) was adjusted by subtracting the number of squares devoid of tissue, and the squares containing NIS-positive areas were counted to calculate the percentage of NIS-positive areas per total tissue core area.

SPECT/CT image reconstruction and quantification

This study included 50 thyroid cancer patients treated with ^{131}I between October 2010 and September 2011 at OSUWMC. Patients ranged in age from 17 to 75 years old and included 14 males and 36 females. Data collection and analysis were conducted under an expedited IRB-approved protocol. Prior to ablation therapy, each patient was administered ^{123}I (2.54 ± 0.07 mCi) to determine RAI uptake 24 hours later via planar imaging of the neck and whole body (Biodex 187-140, Atomlab 950 V.3.36, 1024 multichannel analyzer), as well as with a SPECT/CT (Symbia T-16; Siemens Medical Solutions, Malvern, PA) of the head and neck. Patients were placed in supine position for scanning that extended from the eyes to the base of the heart, with an acquisition time of 60 seconds per step and a reconstructed slice width of 3 mm. Data were processed using the Flash 3D algorithm and sent to Syngo MultiModality Workplace (Siemens). Each patient's bilateral parotid and submandibular gland counts were calculated using three-dimensional (3D) regions of interest (ROI) measurements with a background count threshold of 10 counts. Total counts per gland were calculated based on data generated from the 3D ROI using mean counts per cm^3 × total salivary gland volume (cm^3).

Statistical analysis

For ratios of ^{123}I accumulation, means ± standard errors (SEs) were calculated, and descriptive plots and correlations were generated. Linear regression models were fit to the log-transformed ratio data with dose, age, and sex as the primary predictors. The presence of two-way interactions was assessed. From the Aprd/Asmd model (ratio of average counts per cm^3 between parotid and submandibular glands) the estimated change with age was estimated with confidence intervals [CI]. Mean statistics were reported with their SEs to reflect their level of precision. A mixed-effects model was applied to the percentage of NIS-positive striated duct data to allow for correlations among observations from the same case. The model included both sex and age (divided into tertiles). Differences between parotid and submandibular glands were estimated with CIs. For basic summary statistics, observations within an organ class for a particular case were first averaged, and then the percentage of NIS-positive areas in the core were then calculated based on the averaged data. All analyses were performed using SAS/STAT software, v9.2 (SAS Institute Inc., Cary, NC).

Results

NIS expression is primarily restricted to the striated ducts of the salivary gland

As depicted in Figure 1A, NIS is highly expressed along the basolateral membrane of striated duct cells with decreased expression of much fewer excretory duct cells. NIS expression is mostly negative in intercalated duct cells with emergence of expression as they transition to striated ducts. This distinct pattern of NIS immunostaining within specific segments of the salivary ductal system does not differ among submandibular, parotid, and minor salivary glands (Fig. 1B). Among 85 normal salivary tissue cores containing striated ducts, 78 (92%) demonstrated 3+ NIS staining in striated ducts, with >75% of the striated duct cells expressing NIS. Intercalated and excretory ducts demonstrated weaker immunoreactivity in fewer duct cells. Among 87 cores containing intercalated ducts, 48 (55%) cores were negative and 36 (41%) demonstrated 1+ or 2+ NIS staining in ≤25% of the intercalated duct cells. Among 14 cores containing excretory ducts, five (36%) cores were negative, and seven (50%) demonstrated 1+ or 2+ in ≤25% of the excretory duct cells. Due to the continuity of salivary ducts, the transition zones from intercalated to striated ducts and striated to excretory ducts are not clearly defined. Nevertheless, NIS expression in salivary ductal cells appears to be abruptly increased during the transition of intercalated to striated ducts and is decreased during the transition of striated to excretory ducts.

The percentage of NIS-positive striated ducts in parotid glands is statistically lower than in submandibular glands

To investigate whether there is a difference in NIS-mediated radionuclide uptake between parotid and submandibular glands, we compared the percentage of NIS-positive duct cells among different salivary glands utilizing a grid superimposed over each NIS-stained normal salivary gland tissue core (Fig. 2A). Of normal salivary tissue cores examined with the presence of striated ducts, the percentage of NIS-positive duct cells in the submandibular glands range from 1.9% to 13.8% with a mean ± SE of 7.5 ± 0.7. In comparison, the percentages in the parotid gland range from 1% to 11.2% with a mean ± SE of 4.6 ± 0.6, and in the minor salivary glands from 0% to 10.2% with a mean ± SE of 4.1 ± 1.3 (Fig. 2B). The determined percentage of NIS-positive cells most likely overestimates the actual percentage of NIS-positive cells in their corresponding salivary glands. This is due, in part, to the composition of the tissue microarray in which areas were selected based on the presence of ductal cells. In addition, some squares on the grid scored as positive for NIS are not entirely occupied by NIS-positive ductal cells. However, we believe that the relative differences in the percentage of NIS-positive cells among different salivary glands are not compromised by overestimation of the percentage of NIS-positive ductal cells. Overall, the percentage of NIS-positive cells in the submandibular gland is significantly higher than that in the parotid gland ($p = 0.0003$). Indeed, the submandibular gland is known to have a greater relative component of striated ducts, where NIS is highly expressed, than the parotid gland (see Fig. 5A below) (5). Further analysis reveals that the percentage of NIS-positive cells decreases with age in the parotid gland, yet slightly increases with age in submandibular glands. This different trend may partially account for the decrease in ratios of average counts per cm^3 between parotid and submandibular glands (Aprd/Asmd) with age, as described below.

Most thyroid cancer patients exhibit greater cumulative radioactivity in parotid glands compared with submandibular glands

Cumulative ^{123}I radioactivity in the parotid and submandibular gland was examined by SPECT/CT imaging 24 hours after ^{123}I administration in 50 thyroid cancer patients. The ratios of cumulative ^{123}I radioactivity counts between parotid and submandibular glands (Cprd/Csmd) range from 0.36 to 6.18 with a mean ± SE of 2.38 ± 0.19. Only 3/50 (6%) patients had a Cprd/Csmd <1. The volume of ROI was used to normalize cumulative radioactivity counts to acquire average cumulative radioactivity counts per cm^3. The ratios of average counts per cm^3 between parotid and submandibular glands, that is, Aprd/Asmd, range from 0.33 to 2.7 with a mean ± SE of 1.19 ± 0.06. Nineteen of 50 (38%) patients had an Aprd/Asmd <1.

As shown in Figure 3A, Cprd/Csmd ratios appear to be positively correlated with Aprd/Asmd ratios (estimated correlation = 0.67). In this study, patients' age ranges from 16 to 75 years with a mean ± SE of 48.6 ± 2.2, and 36/50 (72%) patients are female. Interestingly, the Aprd/Asmd ratios decrease as ages increase (Fig. 3B), but there is no significant difference between males and females. Of note, the ratio of Cprd/Csmd or Aprd/Asmd not only reflects the difference in NIS-mediated ^{123}I uptake, but also the rate of saliva clearance between parotid gland and submandibular gland.

NIS expression is reduced in sialoadenitis and absent in most salivary gland neoplasms

As summarized in Figure 4A, NIS expression in striated ducts is reduced in inflamed salivary glands and is absent in the majority of salivary gland neoplasms. Among 39 salivary tissue cores with sialoadenitis, 7 (18%) were negative, and only 17 (44%) demonstrated 3+ staining, with most exhibiting

NIS expression in <75% of the striated duct cells. In inflamed salivary gland tissue, NIS reduction was often heterogeneous among cells within the same striated duct (Fig. 4B-i) or among different striated ducts within proximity (Fig. 4B-ii). NIS reduction was particularly evident in striated duct cells undergoing goblet cell metaplasia (Fig. 4B-ii), and was absent in lymphoepithelial lesions. Otherwise it was difficult to attribute differences in NIS expression to the degree of lymphocyte infiltration or fibrosis surrounding striated ducts.

NIS expression was absent in the vast majority of benign and malignant neoplasms of ductal origin. Benign tumors evaluated included pleomorphic adenoma ($n=10$), Warthin's tumor ($n=6$), monomorphic adenoma ($n=4$), papillary oncocytic cystadenoma ($n=2$), and canalicular adenoma ($n=1$). In Warthin's tumor, NIS expression remains with 2+ to 3+ staining intensity in the majority of tumor cells (Fig. 4B-iii). One of two papillary oncocytic cystadenomas also expressed NIS but only with 1+ staining intensity in the minority of

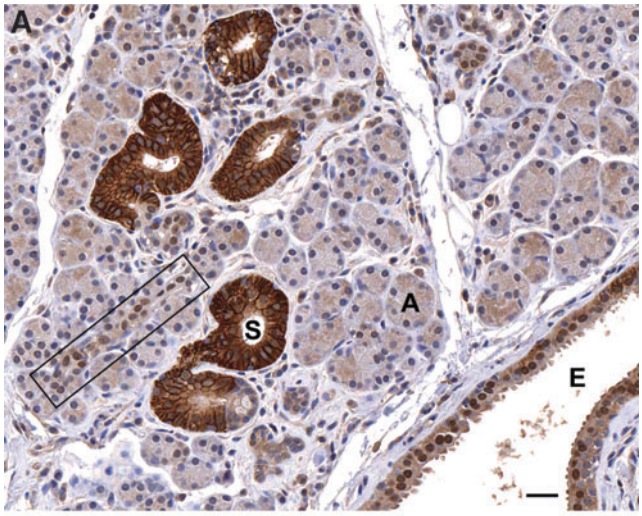

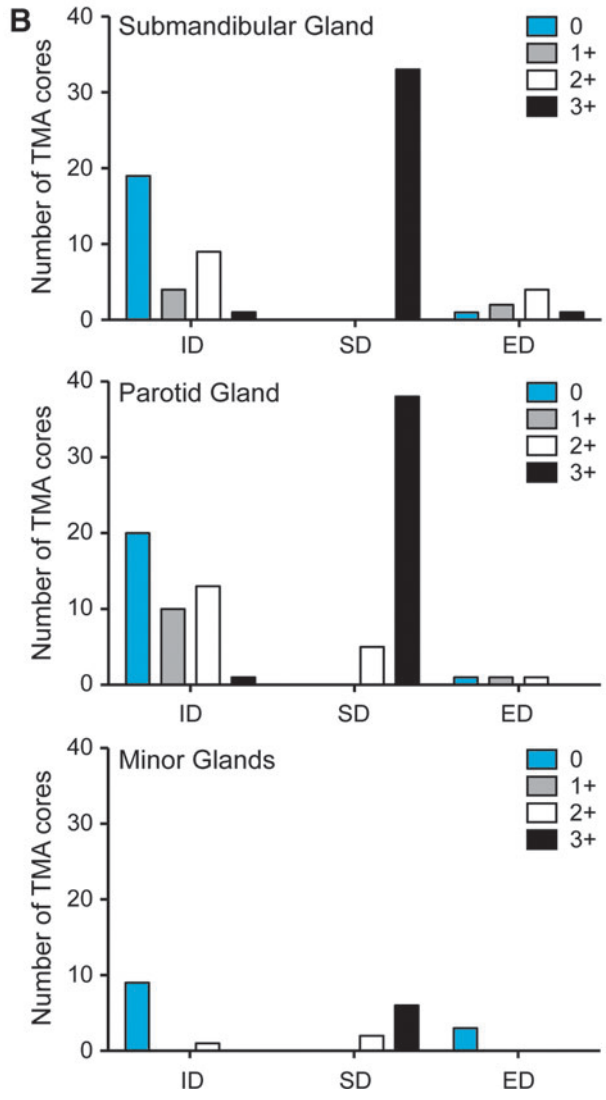

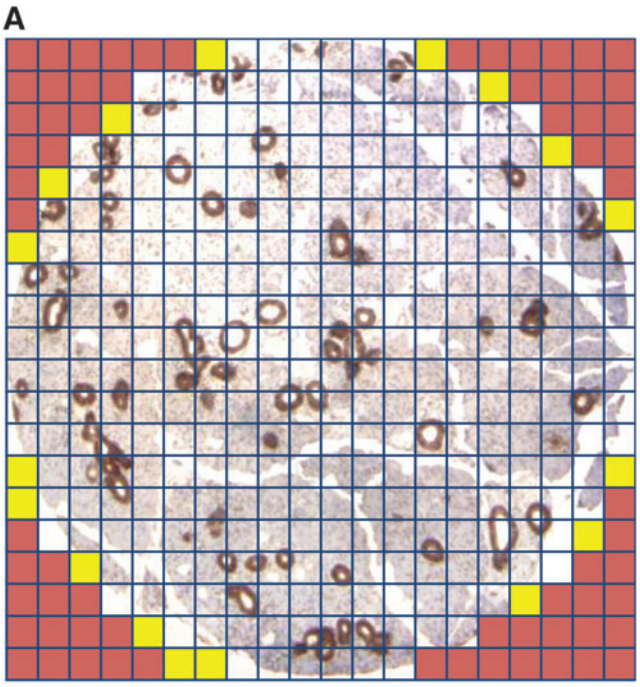

FIG. 2. Percentage of NIS-positive striated duct cells in normal human salivary gland cores. **(A)** A 20×20 grid with 400 squares was superimposed over each tissue core. The number of squares overlying the core area (333) was adjusted by subtracting the number of squares devoid of tissue (yellow squares). Squares containing NIS-positive ducts were counted and percentages of NIS-positive areas per total tissue area were calculated. (*continued*)

FIG. 1. Sodium/iodide symporter (NIS) expression is primarily restricted to striated ducts in human salivary glands. **(A)** NIS is expressed at a high level along basolateral membranes of striated duct cells (S), with fewer intercalated (rectangle) and excretory (E) duct cells demonstrating lower NIS levels. Acinar (A) cells do not express NIS. Anti-human NIS antibody, avidin-biotin complex, DAB chromogen, hematoxylin counterstain, bar = 25 μm. **(B)** Distribution and intensity of NIS immunoreactivity among intercalated (ID), striated (SD), and excretory (ED) ductal cells in normal human submandibular, parotid, and minor salivary glands. NIS expression is greater and more frequent in striated ducts, regardless of gland type.

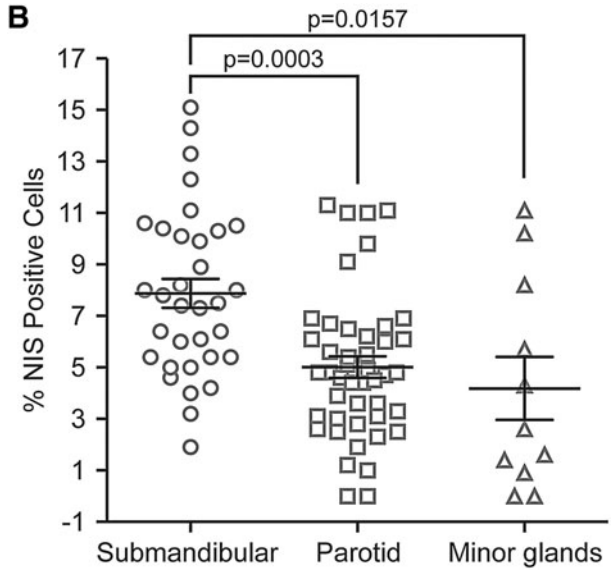

FIG. 2. (*continued*) **(B)** The percentage of NIS-positive striated duct cells is significantly greater in submandibular glands compared to parotid and minor salivary glands.

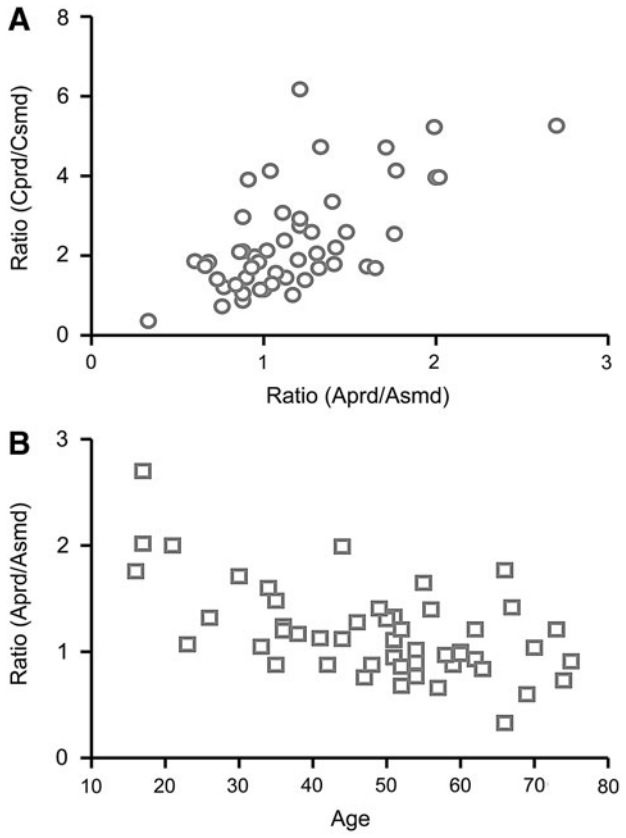

FIG. 3. Salivary ^{123}I accumulation quantified by single-photon emission computed tomography (SPECT)/CT imaging in thyroid cancer patients prior to ^{131}I treatment. **(A)** Ratios of ^{123}I radioactivity counts in parotid (Cprd) and submandibular (Csmd) glands are positively correlated with radioactivity counts normalized by volume of interest in parotid (Aprd) and submandibular (Asmd) glands, with a best-fit slope of 1.9 ± 0.3. The dotted line represents slope = 1. **(B)** Aprd/Asmd ratios are negatively correlated with patient age.

tumor cells (<10%). Malignant neoplasms, including adenoid cystic carcinoma ($n = 5$), ductal carcinoma ($n = 4$), carcinoma ex pleomorphic adenoma ($n = 3$), mucoepidermoid carcinoma ($n = 3$), and polymorphous low-grade adenocarcinoma ($n = 3$), were mostly negative for NIS. However, NIS expression was 2+ in one in three mucoepidermoid carcinomas (Fig. 4B-iv) and 1+ in one in five adenoid cystic carcinomas. Note that two tumor cores were examined from each case, except one case of pleomorphic adenoma, carcinoma ex pleomorphic adenoma, mucoepidermoid carcinoma, and polymorphous low-grade adenocarcinoma, in which only one tumor core was generated and examined.

NIS expression is retained in salivary tumors derived from striated ducts

Among the three major salivary glands, the parotid gland has the highest proportion of ductal components, yet the submandibular gland has the highest proportion of striated duct cells (Fig. 5A) (5,12). Tumors derived from striated ducts, such as Warthin's tumor, retained NIS expression albeit at reduced levels. NIS expression was also retained in one in three mucoepidermoid carcinomas derived from excretory ducts, and one in five adenoid cystic carcinomas derived from intercalated ducts. Taken together, NIS expression appears to be absent in most tumors, albeit NIS expression may remain present in some tumors originating from NIS-positive ductal cells.

NIS expression in Warthin's tumors corroborates their reported scintigraphic characteristics, that is, accumulation of RAI and ^{99m}Tc-pertechnetate (13,14). Co-existence of Warthin's tumor in thyroid cancer patients may present as a potential source of diagnostic error for metastasis. A 66-year-old female with a history of follicular thyroid cancer presented post-thyroidectomy with postsurgical hypothyroidism. Her baseline thyroglobulin and thyroglobulin antibody levels were undetectable prior to undergoing a ^{123}I whole-body scan for assessment of thyroid tissue in the neck and/or metastatic disease. Focal areas of increased ^{123}I uptake were identified in the bilateral superior neck regions (Fig. 5B-i). On SPECT/CT evaluation, these bilateral foci were suggestive of lymph nodes in or around the parotid salivary gland (Fig. 5B-ii–iv). The cytologic diagnosis of fine-needle aspirates from these bilateral discrete foci was oncocytic neoplasm, suspicious for Warthin's tumor. Accordingly, the patient was not subjected to additional ^{131}I treatment.

Discussion

In this study, we found that NIS expression in salivary ductal cells is tightly modulated among the three components of salivary ducts; that is, NIS expression is primarily restricted to striated ducts. NIS expression in striated ducts is heterogeneously decreased in inflamed salivary glands and remains, albeit at reduced levels, in tumors derived from striated ducts. Accordingly, NIS expression in striated ducts could be modulated by signals conferring the striated duct phenotype, cytokines/microenvironments elicited via inflammation, and molecular events underlying tumor formation. The discordance between the greater percentage of NIS-positive striated duct cells and the lower cumulative ^{123}I radioactivity in submandibular versus parotid glands supports a higher clearance rate of saliva secretion in submandibular glands. Finally, the

finding that cumulative ^{131}I radioactivity in submandibular gland increases with age suggests that the incidence of ^{131}I-induced submandibular dysfunction may be increased in older patients.

Although salivary secretion decreases with age (15,16), the submandibular gland is known to have a higher spontaneous saliva secretion rate than the parotid gland. Indeed, 62% of thyroid cancer patients had an Aprd/Asmd ratio >1 at 24 hours post ^{123}I administration, despite a greater percentage of NIS-positive cells in the submandibular gland. Based on studies of external radiation-induced salivary gland damage, it is widely accepted that the parotid gland is more radiosensitive than the submandibular gland. This is attributed in part to its acinar phenotype, composed entirely of serous cells, which are susceptible to membrane lipid peroxidation, resulting in inhibited water excretion (17). While the

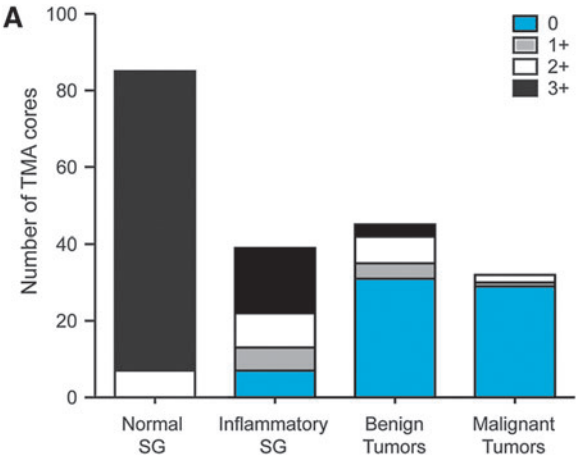

FIG. 4. NIS expression is reduced in inflamed and neoplastic human salivary glands. **(A)** NIS expression in striated ducts is decreased in inflammatory salivary glands, as well as in benign and malignant neoplasms of ductal origin. **(B)** NIS immunoreactivity in inflamed **(i, ii)** and neoplastic **(iii, iv)** salivary tissue. NIS expression is variably decreased in striated ducts (S) of chronically inflamed salivary glands **(i, ii)**, particularly in ducts demonstrating goblet metaplasia (arrows). Neoplastic cells of Warthin's tumor **(iii)** and mucoepidermoid carcinoma **(iv)** demonstrate lower NIS level, with immunostaining intensity of 2+ and 1+, respectively. Anti-human NIS antibody, avidin-biotin complex, DAB chromogen, hematoxylin counterstain, bars = 25 μm. F, periductal fibrosis; L, lymphocytic inflammation.

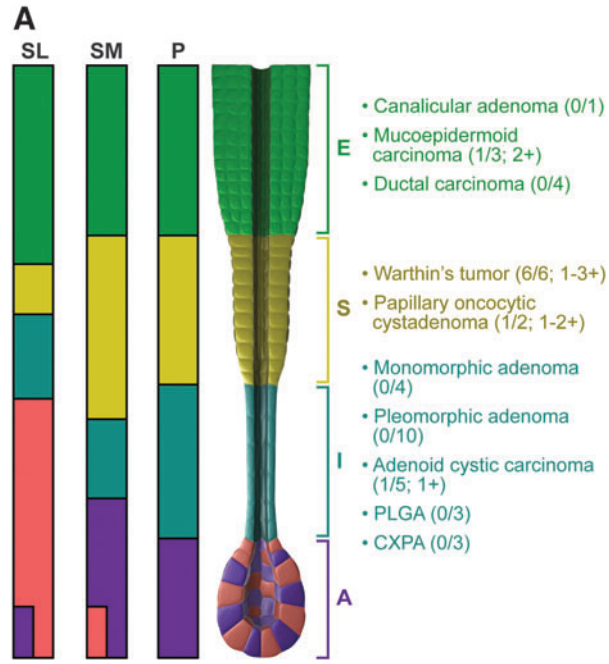

FIG. 5. NIS expression in salivary gland tumors of different ductal cell origins. **(A)** Human salivary gland tumors evaluated for NIS expression correlated with intercalated duct (I), striated duct (S), or excretory duct (E) origin. Relative proportions of acinar and various ductal components are color coded for human parotid (P), submandibular (SM), and sublingual (SL) salivary glands. Numbers in parentheses correspond to cases staining positively for NIS/total cases with corresponding stain intensity. Most tumors expressing NIS are of striated duct origin. A, acinar cells; PLGA, polymorphous low-grade adenocarcinoma; CXPA, carcinoma ex pleomorphic adenoma. Modified from Refs. (5,12). (*continued*)

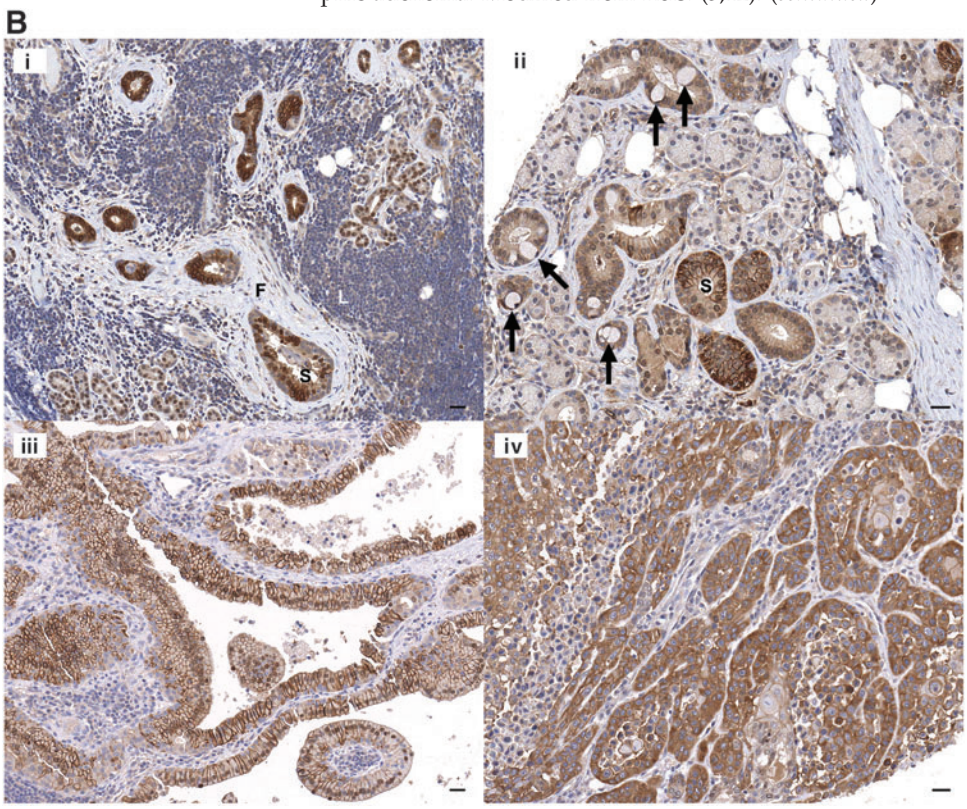

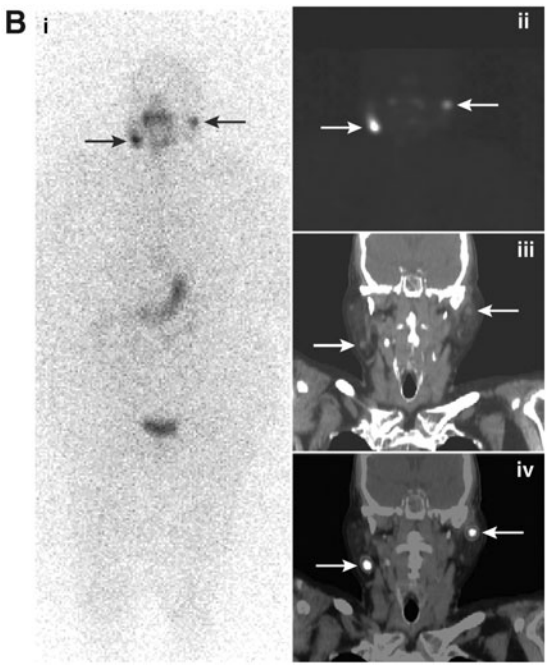

FIG. 5. (*continued*) **(B)** Radioactive iodine uptake in Warthin's tumor. ^{123}I uptake (black and white arrows) bilaterally in the neck of a 66-year-old, female, follicular thyroid cancer patient post-thyroidectomy. **(i)** Whole body scan; **(ii–iv)** SPECT/CT images: SPECT **(ii)**; CT **(iii)**; fused **(iv)**. Areas of uptake corresponded to oncocytic neoplasms of parotid glands, suspicious for Warthin's tumor.

submandibular gland is a mixture of serous- and mucous-secreting acini, serous-secreting acini predominate (5). In addition, the relative acinar component in the submandibular gland is greater than in the parotid gland (5). Accordingly, radiosensitivity in serous acinar cells may not fully explain the prevalence of parotid dysfunction in ^{131}I-treated patients.

In contrast to patients with head and neck cancer who receive external radiation, we believe that ductal cells rather than acinar cells are the primary targets of ^{131}I damage in patients with thyroid cancer. This is supported by patients treated with ^{131}I who often suffer from obstructive symptoms reflecting ductal damage and xerostomia, which is contingent on the extent of acinar damage developed over time (7). ^{131}I taken up by striated duct cells accumulates in ductal lumina prior to clearance via saliva secretion. Accordingly, acinar cells in proximity to ductal lumina may also be subjected to ^{131}I damage as the maximal range of β particles emitted by ^{131}I that cause nuclear damage is about 3.45 mm (18). However, acinar cells may atrophy after prolonged and severe obstruction of salivary ducts (19).

The decreased and heterogenous NIS expression noted in numerous cases of sialoadenitis offers insight into the functional alterations observed in salivary glands following ^{131}I treatment. Patients who suffer from recurrent and chronic ^{131}I-induced sialoadenitis are characterized by minimal uptake and no secretory clearance when evaluated with ^{99m}Tc-pertechnetate (TPT) time activity graph (7). The inability to uptake TPT, a known NIS substrate, is most likely due to reduced NIS in inflamed glands. The failure of secretory clearance of TPT reflects underlying ductal cell damage. If we could identify the factors that contribute to loss of NIS expression in a subset of striated ducts in inflamed salivary tissues, we may be able to devise novel strategies to shut down NIS expression selectively in striated ducts during RAI treatment to prevent ^{131}I-induced salivary gland damage.

Taken together, we have further investigated NIS expression in various ductal components of the salivary gland, documented decreased NIS expression in sialoadenitis, and linked NIS expression in salivary gland neoplasms to a subset of ductal cells. Future studies elucidating the mechanisms of NIS modulation in the transitions between intercalated to striated ducts and striated to excretory ducts, as well as in aging and inflamed salivary glands, will facilitate the development of novel strategies to preserve salivary gland function in ^{131}I-treated thyroid cancer patients.

Acknowledgments

This work was supported in part by NIH P01 CA124570. We thank Mr. Tim Vojt in Biomedical Media, College of Veterinary Medicine, for medical illustration and image processing; and Ms. Viy McGaughy and Ms. Susie Jones in the Pathology Core Facility for immunohistochemistry services.

Author Disclosure Statement

The authors declare that they have no commercial associations that might create a conflict of interest in connection with this article.

References

1. Jhiang SM, Cho JY, Ryu KY, DeYoung BR, Smanik PA, McGaughy VR, Fischer AH, Mazzaferri EL 1998 An immunohistochemical study of Na^+/I^- symporter in human thyroid tissues and salivary gland tissues. Endocrinology **139:**4416–4419.
2. Spitzweg C, Joba W, Schriever K, Goellner JR, Morris JC, Heufelder AE 1999 Analysis of human sodium iodide symporter immunoreactivity in human exocrine glands. J Clin Endocrinol Metab **84:**4178–4184.
3. Vayre L, Sabourin JC, Caillou B, Ducreux M, Schlumberger M, Bidart JM 1999 Immunohistochemical analysis of Na^+/I^- symporter distribution in human extra-thyroidal tissues. Eur J Endocrinol **141:**382–386.
4. Bruno R, Giannasio P, Ronga G, Baudin E, Travagli JP, Russo D, Filetti S, Schlumberger M 2004 Sodium iodide symporter expression and radioiodine distribution in extra-thyroidal tissues. J Endocrinol Invest **27:**1010–1014.
5. Ross MH, Pawlina W 2006 Digestive system I: oral cavity and associated structures. In: Ross MH, Pawlina W (eds) Histology: A Text and Atlas with Correlated Cell and Molecular Biology. Fifth edition. Lippincott Williams & Wilkins, Baltimore, MD, pp 476–517.
6. Venturi S, Venturi M 2009 Iodine in evolution of salivary glands and in oral health. Nutr Health **20:**119–134.
7. Mandel SJ, Mandel L 2003 Radioactive iodine and the salivary glands. Thyroid **13:**265–271.
8. Newkirk KA, Ringel MD, Wartofsky L, Burman KD 2000 The role of radioactive iodine in salivary gland dysfunction. Ear Nose Throat J **79:**460–468.

9. Van Nostrand D 2011 Sialoadenitis secondary to ^{131}I therapy for well-differentiated thyroid cancer. Oral Dis **17:**154–161.
10. Liu B, Huang R, Kuang A, Zhao Z, Zeng Y, Wang J, Tian R 2011 Iodine kinetics and dosimetry in the salivary glands during repeated courses of radioiodine therapy for thyroid cancer. Med Phys **38:**5412–5419.
11. Malpani BL, Samuel AM, Ray S 1995 Differential kinetics of parotid and submandibular gland function as demonstrated by scintigraphic means and its possible implications. Nucl Med Commun **16:**706–709.
12. Martínez-Madrigal F, Bosq J, Casiraghi O 1997 Major Salivary Glands. In: Sternberg SS (ed) Histology for Pathologists. Second edition. Lippincott Williams & Wilkins, Philadelphia, PA, pp 405–429.
13. Murata Y, Yamada I, Umehara I, Okada N, Shibuya H 1998 Diagnostic accuracy of technetium-99m-pertechnetate scintigraphy with lemon juice stimulation to evaluate Warthin's tumor. J Nucl Med **39:**43–46.
14. Weinstein GS, Harvey RT, Zimmer W, Ter S, Alavi A 1994 Technetium-99m pertechnetate salivary gland imaging: its role in the diagnosis of Warthin's tumor. J Nucl Med **35:**179–183.
15. Dodds MW, Johnson DA, Yeh CK 2005 Health benefits of saliva: a review. J Dent **33:**223–233.
16. Yeh CK, Johnson DA, Dodds MW 1998 Impact of aging on human salivary gland function: a community-based study. Aging (Milano) **10:**421–428.
17. Konings AW, Coppes RP, Vissink A 2005 On the mechanism of salivary gland radiosensitivity. Int J Radiat Oncol Biol Phys **62:**1187–1194.
18. L'Annunziata MF 2003 Nuclear radiation, its interaction with matter and radioisotope decay. In: L'Annunziata MF (ed) Handbook of Radioactivity Analysis. Second ed. Academic Press, San Diego, CA, pp 1–121.
19. Cotroneo E, Proctor GB, Carpenter GH 2010 Regeneration of acinar cells following ligation of rat submandibular gland retraces the embryonic-perinatal pathway of cytodifferentiation. Differentiation **79:**120–130.

Address correspondence to:
Sissy M. Jhiang, PhD
The Ohio State University
304 Hamilton Hall, 1645 Neil Ave.
Columbus, OH 43210-1218

E-mail: jhiang.1@osu.edu